Atmospheric
Chemistry
and Physics

Supplement of

Re-evaluating the reactive uptake of HOBr in the troposphere with implications for the marine boundary layer and volcanic plumes
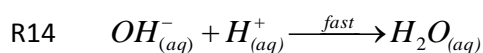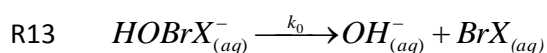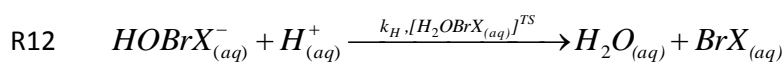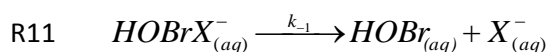
T. J. Roberts et al.

Correspondence to: T. J. Roberts (tjardaroberts@gmail.com)

S1 The kinetics of HOBr+X- according to the general acid assisted mechanism

The reaction of HOBr with X^- in acidic aerosols occurs according to the general-acid assisted mechanism (Eigen and Kustin, 1962), summarized in Section 3.1 in the main text (reactions R10-R14). A parameterisation of the rate of reaction of $HOBr_{(aq)}$ in terms of a pH-dependent second-order rate constant (k^{II}) is then used to calculate reactive uptake coefficients for HOBr under laboratory conditions, and for acidified sea-salt aerosol in the marine environment and in volcanic plumes (E6, main text, Section 3 and 4).

Here, the expression for k^{II} (E6) is derived according to the reaction mechanism, in terms of the underlying rate constants k_1, k_{-1}, k_0 and k_H.

R10 $\quad HOBr_{(aq)} + X^-_{(aq)} \xrightarrow{\;k_1\;} HOBrX^-_{(aq)}$

R11 $\quad HOBrX^-_{(aq)} \xrightarrow{\;k_{-1}\;} HOBr_{(aq)} + X^-_{(aq)}$

R12 $\quad HOBrX^-_{(aq)} + H^+_{(aq)} \xrightarrow{\;k_H,[H_2OBrX_{(aq)}]^{TS}\;} H_2O_{(aq)} + BrX_{(aq)}$

R13 $\quad HOBrX^-_{(aq)} \xrightarrow{\;k_0\;} OH^-_{(aq)} + BrX_{(aq)}$

R14 $\quad OH^-_{(aq)} + H^+_{(aq)} \xrightarrow{\;fast\;} H_2O_{(aq)}$
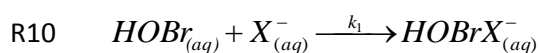
The combination of R10-R14 leads to ES1. Assuming [HOBrX$^-_{(aq)}$] is in steady state leads to ES2.

ES1

$$\frac{d[HOBrX^-_{(aq)}]}{dt}$$
$$= k_1 \cdot [HOBr_{(aq)}] \cdot [X^-_{(aq)}] - k_{-1} \cdot [HOBrX^-_{(aq)}] - k_H \cdot [HOBrX^-_{(aq)}] \cdot [H^+_{(aq)}] - k_0 \cdot [HOBrX^-_{(aq)}]$$
$$= 0$$

ES2 $\quad [HOBrX^-_{(aq)}] = \dfrac{k_1 \cdot [HOBr_{(aq)}] \cdot [X^-_{(aq)}]}{k_{-1} + k_0 + k_H \cdot [H^+_{(aq)}]}$

The rate of reaction of $HOBr_{(aq)}$ is equal to the rate of production of $BrX_{(aq)}$, given by ES3. Substitution of the equation for [HOBrX$^-_{(aq)}$], ES2, into the rate equation ES3, yields ES4, enabling the second-order rate constant, k^{II}, to be defined in terms of k_1,k_0,k_H and [H$^+_{(aq)}$], E6.

ES3 $\quad -\dfrac{d[HOBr_{(aq)}]}{dt} = \dfrac{d[BrX_{(aq)}]}{dt} = k_H \cdot [HOBrX^-_{(aq)}] \cdot [H^+_{(aq)}] + k_0 \cdot [HOBrX^-_{(aq)}]$

ES4

$$\frac{d[BrX_{(aq)}]}{dt} = \left(k_H \cdot [H^+_{(aq)}] + k_0\right) \cdot \frac{k_1 \cdot [HOBr_{(aq)}] \cdot [X^-_{(aq)}]}{k_{-1} + k_0 + k_H \cdot [H^+_{(aq)}]}$$

$$= \frac{k_1 \cdot \left(k_H \cdot [H^+_{(aq)}] + k_0\right)}{k_{-1} + k_0 + k_H \cdot [H^+_{(aq)}]} \cdot [HOBr_{(aq)}] \cdot [X^-_{(aq)}]$$

E6

$$k^{II} = \frac{k_1 \cdot \left(k_0 + k_H \cdot [H^+_{(aq)}]\right)}{k_{-1} + k_0 + k_H \cdot [H^+_{(aq)}]}$$

S2. Calculation of HOBr reactive uptake coefficients

The equation to calculate the HOB reactive uptake coefficient, γ_{HOBr}, is given in equation ES6. Parameters within this equation were defined as follows.

ES6
$$\frac{1}{\gamma_{HOBr}} = \frac{1}{\alpha_{HOBr}} + \frac{v_{HOBr}}{4 \cdot H^*_{HOBr} \cdot R \cdot T \cdot \sqrt{D_{l,HOBr} \cdot k^I}} \cdot \frac{1}{\coth\left[\dfrac{r}{l}\right] - \dfrac{l}{r}}$$

The accommodation coefficient, α_{HOBr} was set to 0.6, following experimental findings by Wachsmuth et al. (2002) who measured accommodation-limited uptake onto $NaBr_{(aq)}$ particles under very low $HOBr_{(g)}$ concentrations. It is assumed that this accommodation coefficient is also representative for acidified $NaCl_{(aq)}$ or $H_2SO_{4(aq)}$ particles in the troposphere.

Temperature, T = 298 K unless otherwise stated, the ideal gas constant R = $8.206 \cdot 10^{-2}$ L atm K^{-1} mol^{-1}. The particle radius, r, was set to r = 1 or r= 0.1 μm, noting the occurrence of both supra- and submicron aerosol in the marine environment and volcanic plumes. The mean molecular velocity of $HOBr_{(g)}$, v_{HOBr}, cm s^{-1} was calculated as $(8 \cdot 8.3144 \cdot T/(0.097 \cdot \pi))^{0.5}$. The diffuso-reactive length-scale, l, describes the typical distance over which reaction occurs, with l = $(D_{l,HOBr}/k^I)^{0.5}$.

The first-order rate constant for aqueous-phase reaction of $HOBr_{(aq)}$, k^I, was defined in terms of the second-order rate constant and the halide concentration, $k^I = k^{II} \cdot [X^-]$. Derivation of k^{II} is described in Supp. Mat Section 1, and its calculation in terms of underlying rate constants is given in the Results. The halide ion concentration was determined using E-AIM and henry's law constants (see Section 3 below). For comparison, uptake coefficients were also calculated using the termolecular approach where $k^I = k_{ter} \cdot [X^-] \cdot [H^+]$.

This study focuses primarily on HOBr reactive uptake under acidic aerosol conditions. In order to account for the dissociation of HOBr under alkaline conditions, we used a modified HOBr rate constant to reflect the dissociation of $HOBr_{aq}$ into BrO^- at high pH. We also assumed $BrO^-_{(aq)}$ is unreactive to $X^-_{(aq)}$. Thus, $k^{II} = k^{II} \cdot [Cl^-_{(aq)}] \cdot [H^+_{(aq)}]/([H^+_{(aq)}]+K_a)$, where the acid dissociation constant is K_a = $2.6 \cdot 10^{-9}$ mol/L (given a pKa for HOBr of 8.59, Nagy and Ashby, 2007), and where the term $[H^+_{(aq)}]/([H^+_{(aq)}]+K_a)$ reflects the fraction of dissolved $HOBr_{(aq)}$ in that remains in the form HOBr.

Two parameterisations for the aqueous-phase diffusion constant for HOBr, D_l, $m^2 s^{-1}$, and the solubility of HOBr, H^*, mol L^{-1} atm^{-1}, for salt solutions and sulphuric acid solutions are used. The former applies for weakly acidified sea-salt aerosol (and is the approach used in studies to date), whereas we consider the latter more appropriate for highly H_2SO_4-acidified sea-salt aerosol and volcanic aerosol.

We use $D_{l,HOBr} = 1.42 \cdot 10^{-5}$ cm^{2}s^{-1} reported by Frenzel et al. (1998) for HOBr diffusion in salt solutions at 291 K, which we apply directly in this study at 298 K. For HOBr diffusion in sulphuric acid solutions, the parameterisation ES7 is used following Klassen et al (1998), where T is the temperature in K, and η is the viscosity of sulfuric acid that given by ES8. $c_{HOBr} = 6.2 \cdot 10^8$ for HOBr, B = 425, n = -1.43, A and T_0 are functions of the wt%H$_2$SO$_4$, (wt): A = 279.4 $-$ 8.8·wt+0.358·wt^2, T_0 = 203-2.6·wt+0.0287·wt^2, where the wt%H$_2$SO$_4$ was determined using the E-AIM thermodynamic model. This parameterisation is valid for 30 wt % to 72 wt % sulfuric acid at temperatures between 220 and 300 K. D_l at lower wt% sulphuric acid (high RH) was estimated by interpolation across the RH and Temperature parameter space, and extrapolation to high RH, yielding a diffusion rate comparable to that of water at very high humidity, i.e. $1.42 \cdot 10^{-5}$ cm^2 s^{-1}.

ES7
$$D_{l,HOBr} = \frac{c_{HOBr} \cdot T}{\eta}$$

ES8
$$\eta = A \cdot T^n \cdot Exp\left[\frac{B}{(T - T_0)}\right]$$

HOBr solubility in weakly acidified sea-salt aerosol is represented using the value for water, $6.1 \cdot 10^3$ M atm^{-1} at 291 K, (Frenzel et al., 1998), which we apply directly to this study at 298 K, consistent with the value of > $1.9 \cdot 10^3$ mol L^{-1} atm^{-1} at 298 K estimated by Blatchley et al., (1991). For HOBr solubility in H$_2$SO$_{4(aq)}$ we use a parameterisation derived by Iraci et al. (2005) based on measurements over 201-252 K in 45-70 wt% H$_2$SO$_4$. In application of this parameterisation, ES9, to the troposphere, we note that the wt%H$_2$SO$_4$ only exceeds 45% in the troposphere if relative humidity is less than ~40-50%. However, Iraci et al. (2005) report that the dependence of solubility, H*, on acid concentration is relatively weak. The parameterisation yields an RH-independent HOBr solubility in sulphuric acid of $4 \cdot 10^2$ M atm^{-1} at 298 K (i.e. an order of magnitude lower than that assumed for water at this temperature), rising to 10^3 M atm^{-1} at 273 K and 10^4 M atm^{-1} at 253 K.

ES9
$$LOG10\left(H^*_{HOBr-H2SO4(aq)}\right) = \frac{2349}{T} - 5.27$$

S3. Application of E-AIM to predict aerosol composition

The E-AIM (Extended Aerosol Inorganic Model) thermodynamic model was used to predict the composition of both acidified sea-salt and volcanic aerosol and in particular the halide concentration, X^-_{aq}. We used E-AIM version I that considers the H^+ - SO_4^{2-} - NO_3^- - Cl^- - Br^- - H_2O system between 200 to 330 K (Carslaw et al. (1995), and model version III that considers the H^+ - NH_4^+ - Na^+ - SO_4^{2-} - NO_3^- - Cl^- - H_2O system at 298K (Clegg et al. (1998)).

Inputs to E-AIM include the temperature, relative humidity and total SO_4^{2-}, Cl^-, Br^-, Na^+, and H^+ in the system defined in mol·m^{-3} volume of atmosphere. Outputs include the number of moles per m^3 of atmosphere of $Na^+_{(aq)}$, $SO_4^{2-}_{(aq)}$, $HSO_3^-_{(aq)}$, $H^+_{(aq)}$, $Br^-_{(aq)}$, $Cl^-_{(aq)}$, $HCl_{(g)}$, $HBr_{(g)}$, the activity coefficients for these species, and the total aerosol volume (cm^3 per m^3). It was thereby possible to calculate the aqueous-phase concentrations and activities of halides and $H^+_{(aq)}$ in the aerosol, in mol L^{-1}.

S3.1 Application of E-AIM to reported experimental conditions:

S3.1.1 HCl-acidified sea-salt aerosol of Abbatt and Wachewsky (1998)

E-AIM model III calculations were performed for HCl-acidified sea-salt aerosol at HCl:NaCl = 0.1:1, 298 K and 80% RH (above deliquescence), according to experimental conditions of Abbatt and Wachewsky (1998). Whilst the experimental aerosol consisted of a bimodal distribution of both large (few μm) and small (<μm) particles, the larger particles (range 1-5 µm diameter, number density $1 \cdot 10^4 - 4 \cdot 10^4$ cm^{-3}, surface area $1 \cdot 10^3$- $6 \cdot 10^3$ cm^2/cm^3) were reported to dominate the observed HOBr uptake. For our calculations we assumed aerosol of 1 µm radius and number density of $1 \cdot 10^4$ cm^{-3}, which yields a surface area density of $1.2 \cdot 10^3$ cm^2/cm^3 and volume density of $4.1 \cdot 10^{-8}$ cm^3/cm^3. This aerosol volume density is approximately equivalent to a pure deliquesced sea-salt concentration of 0.2 µmoles/m^3 Na at 76% RH and 298 K according to E-AIM. Addition of 0.02 µmoles/m^3 HCl (HCl:NaCl = 0.1:1) yields a predicted aerosol composition with activities of 6.6 Mol L^{-1} for $Cl^-_{(aq)}$ and 2.3 Mol L^{-1} for $H^+_{(aq)}$ (equivalent to a pH of -0.3) for RH = 76%. As might be expected, acidification of $NaCl_{(aq)}$ aerosol by HCl leads to an increased acidity without causing a significant reduction in $Cl^-_{(aq)}$ concentration through acid-displacement (given the use of HCl as the acidifying agent).

S3.1.2 H$_2$SO$_4$-acidified sea-salt aerosol of Pratte and Ross (2006)

E-AIM model III calculations were performed for H$_2$SO$_4$-acidified sea-salt aerosol at H$_2$SO$_4$:NaCl = 1.45:1, and 50 and 80% RH, to predict aerosol composition under the experimental conditions of Pratte and Rossi (2006), where the E-AIM model III temperature of 298.15 K is close to the reported experimental conditions of 296 K. An estimated sea-salt concentration of 8 µmol/m^3 Na was

assumed, based on the product of the NaCl molarity (e.g. 2.9 M at 70% RH) initially estimated by Pratte and Rossi (2006) and the reported measured aerosol volume density ($2.7 \cdot 10^{-9}$ cm^3/cm^3). To reach the reported experimental H_2SO_4:NaCl = 1.45:1, an additional 11.6 $\mu M/m^3$ H_2SO_4 was added to the E-AIM input. For simplicity the same input estimate is used for E-AIM calculations across all RH.

The output of our E-AIM calculations gives good general agreement between the predicted E-AIM aerosol volume density (e.g. $0.67 \cdot 10^{-9}$, $2.2 \cdot 10^{-9}$ and $5.5 \cdot 10^{-9}$ $cm^3 cm^{-3}$ at RH = 40, 70 and 90%, respectively) to that reported from their experimental observations ($1.01 \cdot 10^{-9}$, $2.7 \cdot 10^{-9}$ and $5.56 \cdot 10^{-9}$ $cm^3 cm^{-3}$ at RH = 40, 70 and 90%, respectively). However, the E-AIM data suggest the aerosol composition differs to that estimated by Pratte and Rossi (2006).

The E-AIM model predicts that $Cl^-_{(aq)}$ concentrations are $6.8 \cdot 10^{-10}$ and $1.5 \cdot 10^{-7}$ moles m^{-3} at 50 and 80 % RH respectively, equivalent to 0.004 M L^{-1} and 0.08 M L^{-1}. The corresponding $HCl_{(g)}$ concentrations are 8.0 and 7.9 μmoles m^{-3}. Thus, E-AIM predicts that the addition of $H_2SO_{4(aq)}$ causes substantial acid-displacement of $HCl_{(g)}$ from the sea-salt under the experimental conditions. The $HCl_{(g)}$ displacement acts to lower the aerosol $Cl^-_{(aq)}$ concentration, and the effect is more pronounced at low relative humidity where wt%H_2SO_4 of the acidic aerosol solution is higher, hence HCl solubility lower.

Pratte and Rossi (2006) did not measure aerosol composition during their experiment, but make the assumption that chloride remained entirely in the aerosol-phase in their discussion of their data, noting that they not detect any $HCl_{(g)}$. However, the predicted $HCl_{(g)}$ concentrations by E-AIM e.g. $\sim 8 \cdot 10^{-6}$ mol m^{-3}, equivalent to $\sim 5 \cdot 10^{12}$ molec cm^{-3} are below the $\sim 2 \cdot 10^{13}$ molec.cm^{-3} detection limit reported by Pratte and Rossi (2006). This can also be shown directly from the aerosol properties estimated by Pratte and Rossi (2006). For example, at the reported aerosol volume of $2.7 \cdot 10^{-9}$ cm^3/cm^3 at 70% RH would yield a maximum $HCl_{(g)}$ concentration if HCl exsolution from the (estimated) 2.9 M L^{-1} NaCl concentration was complete, of $2.9 \cdot 10^{-3} \cdot 2.7 \cdot 10^{-9} \cdot (6.023 \cdot 10^{23})$ = $4.7 \cdot 10^{12}$ molec.cm^{-3}, i.e. below their reported detection limit.

S3.2 E-AIM application to a progressively H_2SO_4-acidified marine aerosol

Because E-AIM model versions cannot predict the composition of aerosol which contains all four components: Na^+, SO_4^{2-}, Br^- and Cl^-, calculations for sea-salt aerosol were performed with E-AIM version III (see composition above), with bromide concentration calculated subsequently. For simplicity we ignore other possible sea-salt ions (e.g. Mg^{2+}, Ca^{2+}, NH_4^+, NO_3^-) therefore our assumed Na:Cl ratio (1:1) is slightly higher than that of actual sea-water (0.4685: 0.5459 = 0.86:1), Wilson (1975). The aerosol $Br^-_{(aq)}$ concentration was then predicted as follows: total Br concentration was

calculated assuming a Br:Na molar ratio corresponding to that of sea-water (0.000842:0.4685 =0.0018), Wilson (1975). The relative concentrations of $HBr_{(g)}$ and $Br^-_{(aq)}$ were described using the effective Henry's solubility for HBr, H^*(ES10). H^* is a function of the acid dissociation constant ($K_a = 10^9$ M, Schweitzer et al., 2000), and $H^+_{(aq)}$ concentration (determined from the E-AIM model output, noting that HBr contributes negligibly to aerosol acidity compared to H_2SO_4). For a closed system, the partitioning between $HBr_{(g)}$ and $Br^-_{(aq)}$ also depends on the total aerosol volume, and was calculated using ES11, (Seinfeld and Pandis, 2006), involving the HBr solubility, H^* (mol L^{-1} atm^{-1}) the total bromine concentration Br in the system (in moles per L^{-1} of air), the gas constant, R defined earlier, Temperature T in Kelvin, and the liquid water content, $w_L \cdot = L \cdot 10^{-6}$, where L is the total aerosol volume density (g/m^3) determined from the E-AIM output (for a specified sea-salt concentration in moles/m^3 and degree of acidification). This 'simple' model sea-salt aerosol composition does not include carbonate buffering (or the effect of other potential impurities such as ammonium). The model aerosol composition is independent of the particle radius, r (which nevertheless is an input parameter to the calculations of the uptake coefficient).

ES10 $\quad H^*_{HBr} = \dfrac{1.3 \cdot 10^9}{K_a} \cdot \left(1 + K_a / [H^+_{(aq)}]\right)$

ES11 $\quad [Br^-_{(aq)}] = H^*_{HBr} \cdot \dfrac{[Br_t] \cdot R \cdot T}{1 + H^*_{HBr} \cdot w_L \cdot R \cdot T}$

General results for a model sea-salt aerosol that undergoes progressive H_2SO_4 acidification are given in Figure S1, based on a single mode sea-salt aerosol, with a PM10 concentration of 10 μg m^{-3} (Seinfeld and Pandis, 2006), which is equivalent to 0.1 μmoles/m^3 Na^+ at 80% RH and 298 K according to E-AIM calculations of $NaCl_{(aq)}$. Having set [Cl] = [Na], the H_2SO_4:Na molar ratio was varied from 0.05 to 400 and E-AIM was used to determine the equilibrium aerosol composition, with bromide and HBr partitioning determined using Henry's law.

The H_2SO_4-acidification induces acid-displacement of $HCl_{(g)}$, which occurs around H_2SO_4:Na ≥ 0.4 for the model aerosol, depleting $Cl^-_{(aq)}$ concentrations. Further addition of $H_2SO_{4(aq)}$ acts to increase the total aerosol volume but does not in fact dilute [$Cl^-_{(aq)}$] given the presence of a $HCl_{(g)}$ reservoir that responds by increased $HCl_{(g)}$ to $Cl^-_{(aq)}$ partitioning. Conversely, acid-displacement of $HBr_{(g)}$ is less effective due to the higher solubility of HBr (e.g. Sander, 1999), and the increasing aerosol volume (as consequence of the additional $H_2SO_{4(aq)}$) acts to dilute $Br^-_{(aq)}$ (as well as $Na^+_{(aq)}$) at high H_2SO_4:Na. Note that in our model aerosol HBr temporarily partitions to the gas-phase upon addition of $H_2SO_{4(aq)}$ but returns to the aqueous-phase at higher H_2SO_4:Na ratios as consequence of the

increasing total aerosol volume. However, in a real marine environment with multiple aerosol modes, bromide might largely remain in the aqueous-phase. In any case, there exists no $HBr_{(g)}$ reservoir at high H_2SO_4:Na ratios; bromide concentrations are diluted but the bromide:sodium ratio in the aerosol still reflects that of sea-salt. In summary, halide concentrations are reduced in H_2SO_4-acidified sea-salt aerosol both by acid-displacement of $HCl_{(g)}$ and by dilution of $Br^-_{(aq)}$ by the additional $H_2SO_{4(aq)}$ volume upon a high degree of H_2SO_4-acidification. Similar HCl-displacement is expected to occur for HNO_3-acidification of sea-salt aerosol, but not for acidification of sea-salt aerosol by HCl.

Figure S1

Gas-aerosol partitioning according to E-AIM thermodynamic model III for a progressively H_2SO_4-acidified model sea-salt aerosol. Temperature is 298 K, relative humidity is 80%. Na concentration was set to $1.3 \cdot 10^{-7}$ moles/m^3, equivalent to a marine environment PM10 of 10 µg/m^3 (Seinfeld and Pandis, 2006) assuming $NaCl_{(aq)}$. Molar concentrations (mole/m^3) of Na^+ (gray), $HCl_{(g)}$ (purple), Cl^-(aq) (pink), Br^-(aq) (light blue), $HBr_{(g)}$ (dark blue) are shown as well as aqueous-phase concentration (mol L^{-1}) as a function of H_2SO_4:Na for $Cl^-_{(aq)}$ (pink), $Br^-_{(aq)}$ (light blue), and $Na^+_{(aq)}$ (grey). Aerosol volume (cm^3/m^3) is shown by black dotted line.
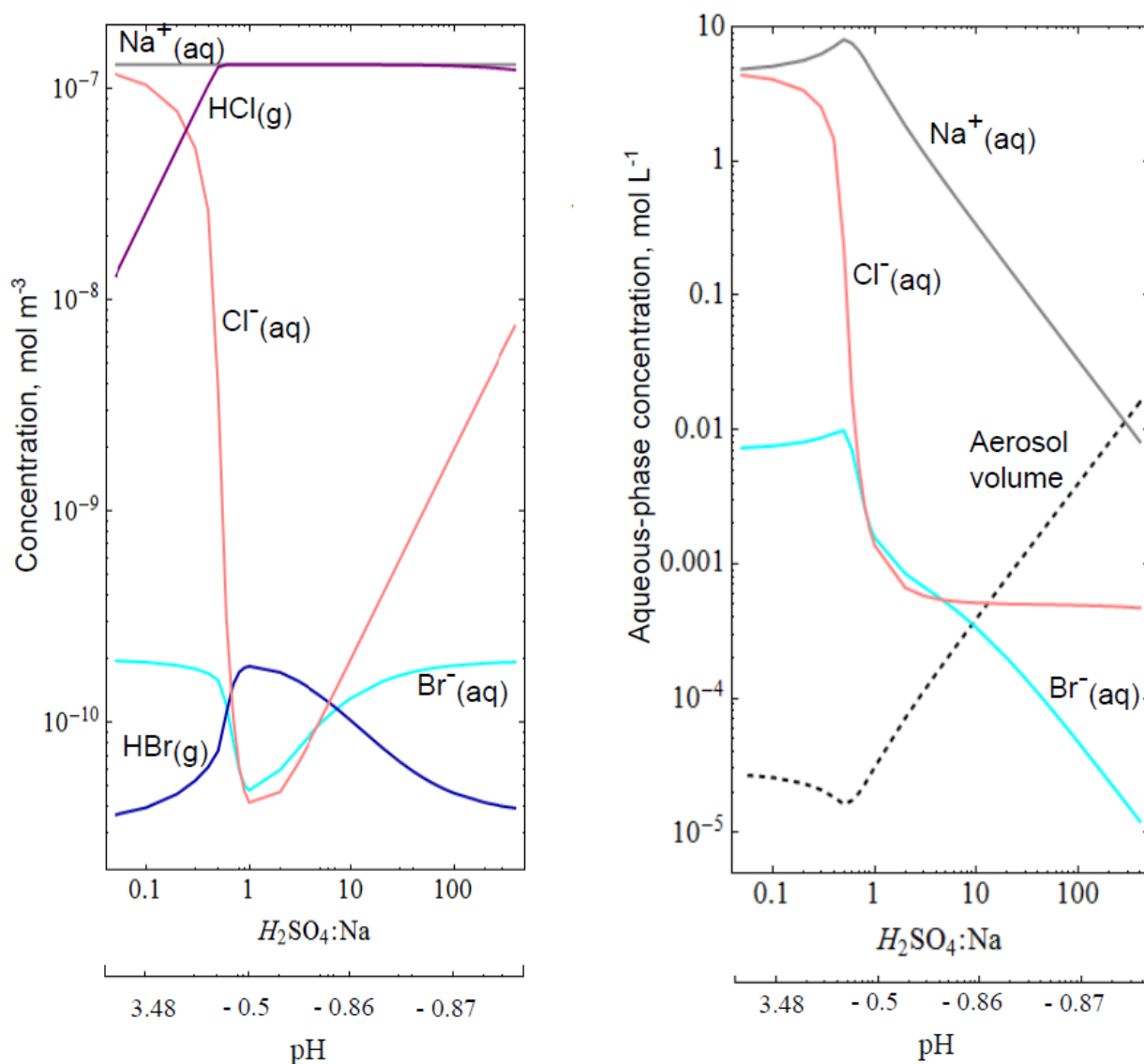
S3.3 Application of E-AIM to volcanic aerosol

E-AIM model version I was used to predict volcanic aerosol composition, particularly concentrations of both $Br^-_{(aq)}$ and $Cl^-_{(aq)}$, over a range of tropospheric RH (0.4-0.99) and temperature (300-230 K). We assumed a volcanic composition of $(SO_2):Cl^-:Br^-: SO_4^{2-}$ of 1:0.5:0.00075:0.01 that is typical for an Arc (subduction zone) volcano such as Etna (note SO_2 simply listed as a reference volcanic gas but is not included in the E-AIM calculation). Anions were balanced by H^+ as the cation. The $SO_4^{2-}:SO_2$ ratio assumed here is based on crater-rim measurements that indicate sulphate:SO_2 molar ratio of ~1:100 (e.g. Mather et al., 2003). This 'quasi-direct' volcanic emission of sulfate is believed to be caused by high-temperature production of SO_3 in the near-vent plume (Mather et al., 2003) followed by lower temperature reaction with H_2O (Roberts et al., 2009). For the abovementioned volcanic emission composition, the absolute concentrations required for the E-AIM input (in moles m^{-3}) were calculated for three different plume strengths equivalent to an SO_2 gas concentration of 30, 3, and 0.3 $\mu mol/m^3$ which is equivalent to approximately 1, 0.1 and 0.01 ppmv SO_2 at 4km altitude (US standard atmosphere).

The predicted aerosol and plume composition for Etna is shown in Figure S2 for two of the three plume dilution scenarios, at three different temperatures. Whilst the Etna emission $((SO_2):HCl:H_2SO_4:HBr$ at molar ratios 1:0.5:0.01:0.00075) contains substantially less HBr than HCl, the higher solubility of HBr relative to HCl leads to relatively similar aqueous-phase concentrations for $Cl^-_{(aq)}$ and $Br^-_{(aq)}$. Both aqueous-phase halide concentrations are more elevated in the stronger (30 $\mu mol/m^3$ SO_2) plume than the dilute (0.3 $\mu mol/m^3$ SO_2) plume scenarios as a consequence of the greater HX partial pressures promoting gas-to-aerosol partitioning in the concentrated plume scenario. Temperature exerts a significant control on $[X^-_{(aq)}]$ through the inverse dependence of halide solubility on temperature. Relative humidity (RH) also exerts a control on $[X^-_{(aq)}]$: the dependence of $[X^-_{(aq)}]$ on RH is initially positive, as HX solubility is greater at higher pH (thus, higher RH). However, in the more concentrated plume scenario the increase in aerosol volume with RH can lead to complete removal of $HX_{(g)}$ followed by dilution of $[X^-_{(aq)}]$. The decline in $[X^-_{(aq)}]$ is more pronounced and occurs earlier for $Br^-_{(aq)}$ than $Cl^-_{(aq)}$ given higher solubility and lower gas-phase concentrations. These declines in $[X^-_{(aq)}]$ are only seen for the strong plume scenario as gas-to-aerosol partitioning is much lower for the dilute plume scenario such that HX is not depleted. The Br^- composition used here for Etna is based on an average volcanic Br/S emission reported by Aiuppa et al. (2005), as used in the modelling study of Roberts et al. (2014), and a factor of two and three lower than that assumed by Roberts et al. (2009) and von Glasow (2010) respectively. Our assumed volcanic aerosol composition also differs to that reported by Martin et al. (2012) in an E-AIM study of

the Masaya volcano emission, due to differences in the volcano-specific gas and aerosol emission, although both of our E-AIM applications predict similar tendencies for aerosol compositional changes as a function of temperature and RH.

Figure S2

Predicted volcanic plume composition for (a) strong plume (30 µmol/m, corresponding to 1 ppmv SO_2 at 4 km in a standard atmosphere) and (b) weak plume (0.3 µmol/m, corresponding to 0.01 ppmv SO_2). Plume halogen composition (in mol m^{-3} of atmosphere) and aqueous-phase composition (in mol L^{-1}) are shown as a function of RH, and for three different temperatures: 293, 263 and 243 K (thick, dashed and dotted lines, respectively), for conditions where aerosol is predicted to be purely in liquid form. Concentrations of $HCl_{(g)}$ (purple), $HBr_{(g)}$ (blue), $Cl^-_{(aq)}$ (pink), $Br^-_{(aq)}$ (cyan) with aqueous phase volume density (cm^3 per m^3, grey lines). For clarity, only 298 K model output is labelled.
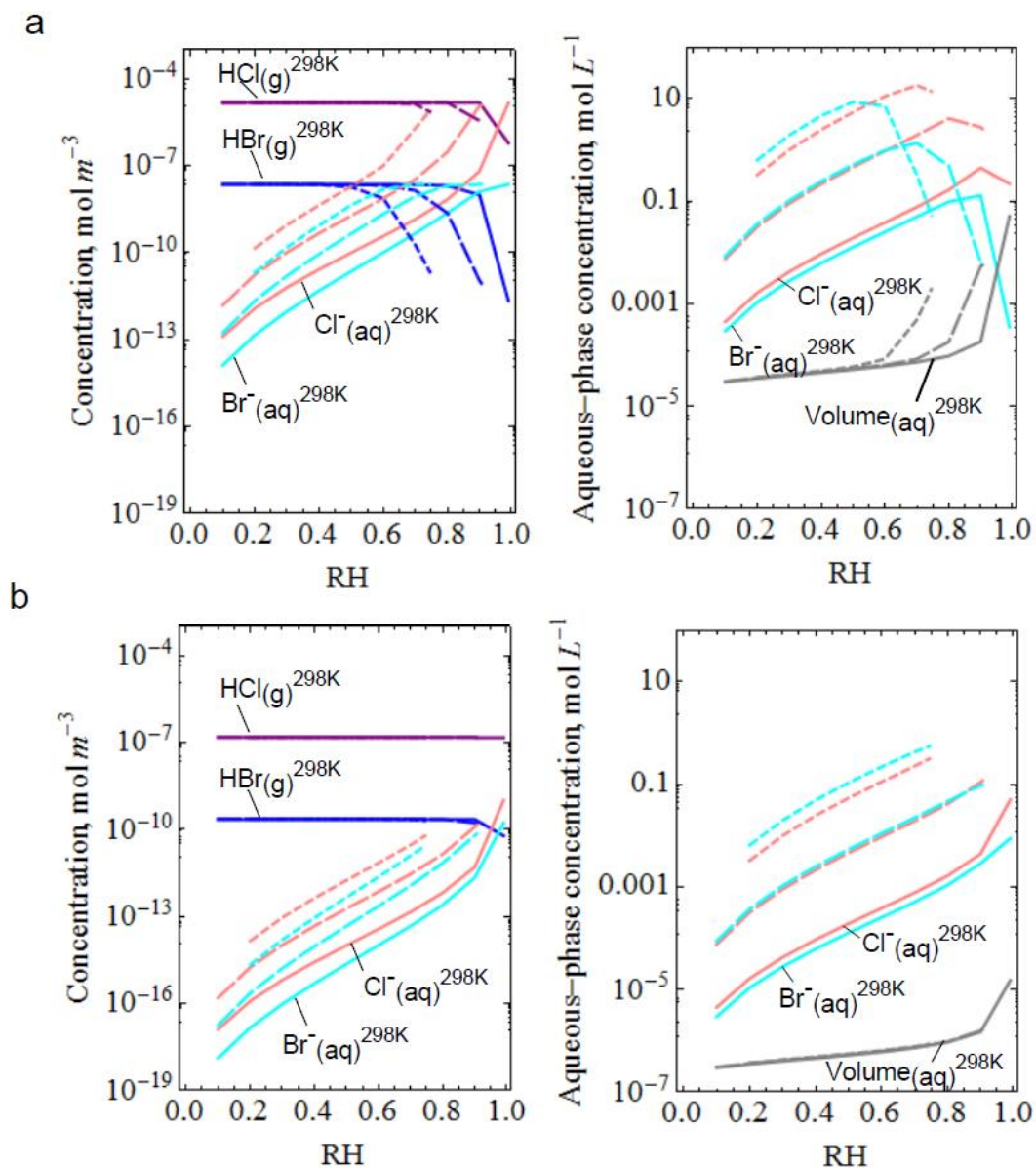
References

Abbatt, J. P. D. and Waschewsky, G. C.G.: Heterogeneous Interactions of HOBr, HNO3, O3, and NO2 with Deliquescent NaCl Aerosols at Room Temperature, J. Phys. Chem. A, 102, 3719–3725, 1998.

Aiuppa, A., Federico, C., Franco, A., Giudice, G., Guierri, S., Inguaggiato TS15 , Liuzzo, M., McGonigle, A. J. S., and Valenza, M.: Emission of bromine and iodine from Mount Etna volcano, Geochem. Geophy. Geosy., 6, Q08008, doi:10.1029/2005GC000965, 2005.

Blatchley, E. R., Johnson, R. W., Alleman, J. E., and McCoy, W. F.: Effective Henry's law constants for free chlorine and free bromine, Water Res., 26, 99–106, 1991.

Carslaw, K. S., Clegg, S. L., and Brimblecombe, P.: A thermodynamic model of the system HCl-HNO3-H2SO4-H2O, including solubilities of HBr, from < 200K to 328 K, J. Phys. Chem., 99, 11557–11574, 1995.

Clegg, S. L., Brimblecombe, P., and Wexler, A. S.: A thermodynamic model of the system H+-NH+4-Na+-SO2−4 -NO−3 -Cl−-H2O at 298.15 K, J. Phys. Chem. A, 102, 2155–2171, 1998

Eigen M. and Kustin K.: The Kinetics of Halogen Hydrolysis, J. Am. Chem. Soc., 1962, 84, 1355–1361, doi:10.1021/ja00867a005, 1962.

Frenzel, A., Scheer, V., Sikorski, R., George, C., Behnke, W., and Zetzsch, C.: Heterogenerous Interconversion Reactions of BrNO2, ClNO2, Br2, and Cl2, J. Phys. Chem. A, 102, 1329–1337, 1998.

Iraci, L. T., Michelsen, R. R., Ashbourn, S. F. M., Rammer, T. A., and Golden, D. M.: Uptake of hypobromous acid (HOBr) by aqueous sulfuric acid solutions: low-temperature solubility and reaction, Atmos. Chem. Phys., 5, 1577–1587, doi:10.5194/acp-5-1577-2005, 2005.

Klassen, J. K., Hu, Z. and Williams, L. R.: Diffusion coefficients for HCl and HBr in 30 wt % to 72 wt % sulfuric acid at temperatures between 220 and 300 K, J. Geophys. Res. 103, 16197-16202, 1998.

Martin, R. S., Wheeler, J. C., Ilyinskaya, E., Braban, C.F., and Oppenheimer, C: The uptake of halogen (HF, HCl, HBr and HI) and nitric (HNO3) acids into acidic sulphate particles in quiescent volcanic plumes, Chem. Geol., 296–297, 19–25, 2012.

Mather, T. A., Allen, A. G., Oppeneheimer, C., Pyle, D. M., and Mc-Gonigle, A. J. S.: Size-Resolved Characterisation of Soluble Ions in the Particles in the Tropospheric Plume of Masaya Volcano, Nicaragua: Origins and Plume Processing, J. Atmos. Chem., 46, 207–237, 2003.

Nagy, P. and Ashby, M. T.: Reactive Sulfur Species: Kinetics and Mechanisms of the Oxidation of Cysteine by Hypohalous Acid to Give Cysteine Sulfenic Acid, J. Am. Chem. Soc., 129, 14082–14091, 2007.

Pratte, P. and Rossi, M. J.: The heterogeneous kinetics of HOBr and HOCl on acidified sea salt and model aerosol at 40–90% relative humidity and ambient temperature, Phys. Chem. Chem. Phys., 8, 3988–4001, 2006.

Roberts, T. J., Braban, C. F., Martin, R. S., Oppenheimer, C., Adams, J. W., Cox, R. A., Jones, R. L., and Griffiths, P. T, Modelling reactive halogen formation and ozone depletion in volcanic plumes, Chem. Geol., 263, 151–163, 2009.

Roberts, T. J., Martin, R. S, and Jourdain, L.: Reactive halogen chemistry in Mt Etna's volcanic plume: the influence of total Br, high temperature processing, aerosol loading and plume dispersion, Atmos. Chem. Phys., 14, 1–19, 2014. doi:10.5194/acp-14-1-2014. in press

Schweizer, F., Mirabel, P., and George, C.: Uptake of hydrogen halides by water droplets, J. Phys. Chem. A, 104, 72–76, 2000.

Seinfeld, J. H. and Pandis, S. N: Atmospheric Chemistry and Physics – From Air Pollution to Climate Change, 2nd Edn., John Wiley & Sons, 2006

von Glasow, R.: Atmospheric Chemistry in Volcanic Plumes, P. Natl. Acad. Sci, USA, 107, 6594–6599, 2010.

Wachsmuth, M., Gäggeler, H. W., von Glasow, R., and Ammann, M.: Accommodation coefficient of HOBr on deliquescent sodium bromide aerosol particles, Atmos. Chem. Phys., 2, 121–131, doi:10.5194/acp-2-121-2002, 2002.

Wilson, T. R. S.: Salinity and the major elements of sea water, in: Chemical Oceanography, 1, 2 Edn., edited by: Riley, J. P. and Skirrow, G., Academic, Orlando FL, 365–413, 1975.